



ELSEVIER

Biochimica et Biophysica Acta 1322 (1997) 77–85

View metadata, citation and similar papers at [core.ac.uk](http://core.ac.uk)

brought to you by CORE

provided by Elsevier - Publisher Connector

## The distance between P680 and Q<sub>A</sub> in Photosystem II determined by ESEEM spectroscopy

H. Hara <sup>a</sup>, S.A. Dzuba <sup>b</sup>, A. Kawamori <sup>a,\*</sup>, K. Akabori <sup>c</sup>, T. Tomo <sup>d,e</sup>,  
K. Satoh <sup>d,e</sup>, M. Iwaki <sup>d</sup>, S. Itoh <sup>d</sup>

<sup>a</sup> Faculty of Science, Kwansei Gakuin University, Nishinomiya 662, Japan

<sup>b</sup> Institute of Chemical Kinetics and Combustion, Russian Academy of Sciences, Novosibirsk 630090, Russian Federation

<sup>c</sup> Faculty of Integrated Arts and Sciences, Hiroshima University, Higashi-Hiroshima 739, Japan

<sup>d</sup> National Institute for Basic Biology, Okazaki 444, Japan

<sup>e</sup> Department of Biology, Faculty of Science, Okayama University, Tsushimanaka Okayama 700, Japan

Received 30 July 1997; accepted 28 August 1997

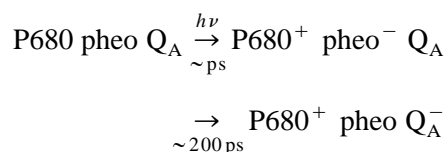
### Abstract

Light induced spin-polarized P680<sup>+</sup>Q<sub>A</sub><sup>-</sup> radical pairs were studied by two pulse electron spin echo envelope modulation (ESEEM) spectroscopy in the cyanide-treated and Zn-substituted Photosystem II core complexes and in the isolated D1-D2-cyt b559 reaction center complexes reconstituted with dibromoisopropyl-*p*-benzoquinone. The observed strong out-of phase ESEEM signals were identified as those of the P680<sup>+</sup>Q<sub>A</sub><sup>-</sup> radical pairs based on the time variation of the transient CW EPR spectra. The shapes of ESEEM spectra were attributed to dipolar *D* and spin exchange *J* interactions in the radical pairs. The values of *D* and *J* were derived from a sine Fourier transformation and the center-to-center distance between P680 and Q<sub>A</sub> was determined to be 27.2 ± 1.0 Å for all three preparations. © 1997 Elsevier Science B.V.

**Keywords:** Photosystem II; P680; Plastoquinone; Spin-polarized radical pair; ESEEM; Dipolar interaction

Light excitation of Photosystem II reaction center (PS II RC) induces the primary charge separation in which the oxidized donor chlorophyll *a* (P680<sup>+</sup>) and

reduced intermediate acceptor pheophytin *a* (pheo<sup>-</sup>) are formed in a few picoseconds [1] at a physiological temperature. Then dark electron transfer to the primary electron acceptor plastoquinone Q<sub>A</sub> forms the secondary radical pair P680<sup>+</sup>Q<sub>A</sub><sup>-</sup> within a few hundred picoseconds as follows,



The P680<sup>+</sup> is then reduced by tyrosine Z (Y<sub>Z</sub>) in a few microseconds, and Q<sub>A</sub><sup>-</sup> is oxidized by the

Abbreviations: PS II, Photosystem II; RC, reaction center; P680, primary electron donor of PS II; Q<sub>A</sub>, primary electron acceptor quinone of PS II; Chl, chlorophyll; cyt, cytochrome; pheo, pheophytin; DBMIB, dibromoisopropyl-*p*-benzoquinone; Mes, 2-morpholinoethanesulfonic acid; PMSF, phenylmethylsulfonyl fluoride; EPR, electron paramagnetic resonance; ESE, electron spin echo; ESEEM, electron spin echo envelope modulation; FWHM, full width at half maximum

\* Corresponding author. Fax: 81 (798) 51-0914; E-mail: kawamori@kwansei.ac.jp

secondary acceptor plastoquinone  $Q_B$  (see for review [2]).

At temperatures below approximately 240 K the electron transfer from  $Q_A^-$  to  $Q_B$  is gradually blocked [3] and that from tyrosine Z to  $P680^+$  is also blocked [4]. Therefore, at low temperatures a major part of the radical pair  $P680^+Q_A^-$  decays in 3–5 ms by the charge recombination between  $P680^+$  and  $Q_A^-$  [4]. A minor portion of  $P680^+$  is reduced either by cyt b559 or by a chlorophyll molecule [5,6]. The electron transfer from cyt b559 or Chl is a slow process [7] compared to the  $P680^+$  reduction by  $Q_A^-$  below 200 K.

EPR signal of  $P680^+$  is usually difficult to be observed because of its short lifetime and high spin–spin relaxation rate [8]. On the other hand,  $Q_A^-$  gives an EPR signal at a cryogenic temperature over a broad field range due to an exchange coupling with the non-heme ferrous iron named as  $Q_A^-Fe^{2+}$  [9]. In a purple bacterial RC,  $Fe^{2+}$  located between  $Q_A$  and  $Q_B$  is connected with  $Q_A$  via a histidine residue [10]. The magnetic coupling between the  $Fe^{2+}$  and  $Q_A^-$  is expected to be removed by depleting the  $Fe^{2+}$  or by substituting zinc for the iron as carried out in the case of the  $P860^+Q_A^-$  radical pair in purple bacterial RC [11–13].

In this report, we have substituted  $Zn^{2+}$  for the  $Fe^{2+}$  in PS II reaction center core complex. This complex composes of D1, D2 cyt b559, 47 kDa and 43 kDa-antenna polypeptides as well as several unpigmented polypeptides [14], which contains all the functional electron transfer molecules including  $Q_A$  and  $Q_B$ . In the core complex, in which Fe was substituted by Zn, the  $P680^+Q_A^-$  recombination showed two decay components with  $t_{1/e}$  of 150  $\mu$ s and 800  $\mu$ s, respectively, at room temperature [15].  $CN^-$ -treatment of the core complex converts the paramagnetic  $Fe^{2+}$  ( $S = 2$ ) state to diamagnetic  $Fe^{2+}$  ( $S = 0$ ) state and the magnetic decoupling produces a narrowed  $Q_A^-$  EPR signal [16]. In the  $CN^-$ -treated PS II, the  $P680^+Q_A^-$  charge recombination rate is expected to be in a similar order as in the Zn-substituted and untreated PS II.

In the D1-D2-cyt b559 PS II RC complex (RC complex), in which  $Q_A^-$  and  $Fe^{2+}$  were already depleted, DBMIB (dibromoisopropyl-*p*-benzoquinone) was recently shown to play the function of  $Q_A^-$  [17]. The  $P680^+(DBMIB)^-$  state was detected within a few ns at 77 K suggesting that DBMIB was fully

reconstituted into the  $Q_A$  binding site. The recombination between  $Q_A^-$  and  $P680^+$  occurred with a  $t_{1/e}$  of about 11 ms at 77 K.

The structure of PS II RC has not yet been analyzed because of difficulty in its crystallization. Therefore, information for the distance between the electron transfer components obtained by the ESE study of dipolar coupling provides valuable insight on the structure and function of PS II.

The method of electron spin echo envelope modulation (ESEEM) spectroscopy of spin-polarized radical pairs has proved to be accurate in the determination of dipolar and exchange couplings, as shown in the studies of bacterial RC [18] and PS I RC [19]. In the ESEEM study of  $P860^+Q_A^-$  radical pair in the bacterial RC, the dipolar and exchange interactions have been determined and the distance between  $P860$  and  $Q_A$  was estimated to be 26 Å [18]. The value of dipolar coupling was in reasonable agreement with the distance between  $P860$  and  $Q_A$  molecules determined from X-ray analysis [20]. The distance between  $P700$  and  $A_1$  (phylloquinone) in the PS I RC, which could not be defined by the X-ray analysis [21], was predicted to be 25 Å by the same method [19].

In this work, we have studied the ESEEM spectra induced by spin–spin interactions between  $P680^+$  and  $Q_A^-$  in the DBMIB-reconstituted RC complex, Zn-substituted and cyanide ( $CN^-$ ) treated PS II core complexes. From the out-of phase ESEEM patterns obtained for the spin-polarized radical pairs, we determined the dipolar and spin exchange interactions, and estimated the distance between  $P680$  and  $Q_A$ .

The spin Hamiltonian of a radical pair system is given by [22],

$$\begin{aligned} \mathcal{H}/\hbar = & g_1 \beta B_0 S_{1z} + g_2 \beta B_0 S_{2z} + S_{1z} \sum A_{1j} I_{1jz} \\ & + S_{2z} \sum A_{2j} I_{2jz} + J \left( \frac{1}{2} - 2 \mathbf{S}_1 \cdot \mathbf{S}_2 \right) \\ & + \frac{D}{2} (3 \cos^2 \theta - 1) [S_z^2 - S(S+1)/3] \quad (1) \end{aligned}$$

where  $\beta$  is the Bohr magneton.  $B_0$  is the static magnetic field ( $\parallel z$  axis of the laboratory frame),  $g_1$  and  $g_2$  are the  $z$ -component of  $g$ -tensor of  $P680^+$  and  $Q_A^-$ ,  $S_1$  and  $S_2$  are each electron spin operator, and  $A_{1j}$  and  $A_{2j}$  are their hyperfine interaction tensors with the  $j$ -th nucleus, respectively.  $I_{1jz}$  and

$I_{2jz}$  are z-component of nuclear spin operators,  $D$  represents the dipolar coupling,  $\theta$  is the angle between the line connecting the radical pair and the direction of the external magnetic field,  $S = S_1 + S_2$  is the resultant spin, and  $J$  is the value of the spin exchange interaction.

The basic spin functions for the spin Hamiltonian  $\mathcal{H}$  are given by  $|T_+\rangle$ ,  $|T_-\rangle$ ,  $|T_0\rangle$  for the triplet state and  $|S\rangle$  for the singlet state.  $|T_0\rangle$  and  $|S\rangle$  are usually mixed into  $|\Phi_a\rangle$  and  $|\Phi_b\rangle$  eigen states by  $S_z\Delta\omega$ .  $\Delta\omega$  is the difference of resonance frequencies for these two spins in the absence of dipolar and exchange interaction.

$$\Delta\omega = (g_{1z} - g_{2z})\beta B_0 + \sum_i A_{1i}m_i - \sum_j A_{2j}m_j \quad (2)$$

Here  $m_{i,j}$  denotes the projection of the  $i,j$ -th nuclear spin onto the z axis for a particular nuclear spin state.

For a spin-polarized radical pair that is originally formed in a singlet state, Tang et al. [22] obtained an analytical expression for the out-of phase primary echo, and presented it by the following relation.

$$F_x(\tau) = \left( \frac{\Delta\omega^2 B^2}{R^4} \right) \sin A\tau [1 - \cos(R\tau)] \quad (3)$$

where  $A = -2D(3\cos^2\theta - 1)/3 + 2J$ ,  $B = D(3\cos^2\theta - 1)/3 + 2J$  and  $R^2 = \Delta\omega^2 + B^2$ . Taking account of the transverse relaxation with a time constant  $T_2$  for four single-quantum transitions,  $|\Phi_a\rangle$  to  $|T_+\rangle$  or  $|T_-\rangle$  and  $|\Phi_b\rangle$  to  $|T_+\rangle$  or  $|T_-\rangle$  [23], the final form of Eq. (3) is modified as follows.

$$F_x(\tau) = \left( \frac{\Delta\omega^2 B^2}{R^4} \right) \sin A\tau [1 - \cos(R\tau)] \exp\left(-\frac{2\tau}{T_2}\right) \quad (4)$$

For randomly oriented samples, Eq. (4) is to be averaged over the angle  $\theta$ .

The D1-D2-cyt b559 RC complex was isolated by the method of Nanba and Satoh [24] from spinach grana thylakoids using Triton X-100 and further purified by electrofocusing in a medium containing digitonin [25]. The quinone reconstitution was performed by incubating the PS II RC complex with DBMIB in a solution containing 50 mM Tris (pH 7.2) and 0.2% digitosulfoxide at 0°C for 30 min in the dark. DBMIB dissolved in dimethylsulfoxide was added to the suspension of the PS II RC complex and mixed with a Vortex mixer for a few seconds immediately after the addition [26]. Under this conditions more than 95%

of the RC complexes can be assumed to be reconstituted with DBMIB [17].

The oxygen evolving PS II particles were isolated from spinach chloroplasts by the method of Kuwabara and Murata [27]. The PS II core complexes were prepared by removing the light-harvesting proteins from the PS II particles, as described in [28]. Tris treatment was performed by incubation of the core complexes on ice in a buffer; 0.8 M Tris-HCl (pH 8.8), 10 mM Na<sub>2</sub>-EDTA, for 30 min under room light.

Removal of non-heme Fe<sup>2+</sup> from the core complex and its substitution by Zn<sup>2+</sup> were carried out by a slightly modified procedure of Klimov et al. [29] in the presence of a serine type proteinase inhibitor (PMSF, 100 μM) in all the process of preparation. The Zn-substituted core complexes were suspended in a solution of 0.4 M sucrose, 10 mM NaCl, 50 mM Mes (pH 6.0). The ratio of substituted Zn was between 70 and 84% per reaction center depending on preparations [15].

CN<sup>-</sup> treatment of the core complex was performed by the method given in [16] with some modification. The buffer used was 340 mM Sorbitol, 10 mM NaCl, 5 mM MgCl<sub>2</sub>, 100 mM Tricine-NaOH (pH 7.8 at 20°C), 10 mM NaHCO<sub>3</sub> and 340 mM KCN. Tris treated core complexes were washed twice by this buffer and then incubated for 90 min at 10°C. After incubation they were washed again with the final buffer solution. All treatments were carried out at approximately 10°C under a dim green safe light. The core complexes were added by 50% (v/v) glycerol and stored at 77 K until use.

To identify the signal origin, transient EPR signals were observed at X-band by using a 1-MHz fast digitizer equipped in the Bruker ESP 300E system. A home-made TE<sub>011</sub> cylindrical cavity with a hole for laser illumination and a cold gas flow system (ESR 900, Oxford Instrument) to regulate the temperature at 80 K were used. The digitizer began to record a spectrum by means of an external trigger at the time 200 μs earlier than laser flash. The samples were illuminated by a Nd:YAG laser (Continuum Surelite I) with a 5 ns pulse FWHM at 532 nm, and a repetition rate of 10 Hz. The microwave power 0.2 mW was used to avoid saturation. 3 G field modulation width at 100 KHz frequency was applied to improve sensitivity.

ESEEM measurements were performed at X-band with a pulsed EPR spectrometer (ESP 380, Bruker) equipped with a cylindrical dielectric cavity (ER4117 DHQ-H, Bruker), and another cold gas flow system (CF935, Oxford Instruments) at 80 K. To acquire the two pulse echo signal, two microwave pulses were created in two separate channels. The pulse length for both pulses was same and equal to 32 ns. To reach the maximum echo amplitude, the phase of the first pulse was set to  $\pi/4$  and that of the second pulse to  $\pi$  [22].

In ESEEM studies, the pulse sequence (laser flash -  $t_0$  - pulse 1 -  $\tau$  - pulse 2 -  $\tau$  - echo) was used. The delay time from the laser flash to the first pulse was set to be  $t_0 = 1 \mu\text{s}$ . A sweep of  $\tau$  was scanned over 75 points with a 16 ns increment and the starting point was at  $\tau = 96$  ns. The signal accumulation number was 200. To study the decay rate of the ESE of the  $\text{P680}^+\text{Q}_\text{A}^-$  radical pair, the following pulse sequence was used (laser flash -  $T$  - pulse 1 -  $\tau$  - pulse 2 -  $\tau$  - echo). In this measurement,  $\tau$  was fixed at 120 ns and the signal amplitude was observed with a various delay time  $T$ . All measurements were repeated with the laser beam being blocked and the obtained signals were used for the background subtraction.

Fig. 1 shows a transient spin-polarized signal around  $g = 2$  observed at 80 K with time constant  $10 \mu\text{s}$  in the  $\text{CN}^-$ -treated core complex. This signal was observed at  $25 \mu\text{s}$  immediately after the laser flash and decayed with a  $t_{1/e}$  about  $30 \mu\text{s}$ . The integrated spectra show a E/A/E/A-like spectrum pattern, where A is an enhanced absorption and E is an emission. These spectra were similar to the E/A/E spectra observed for the radical pair  $\text{P860}^+\text{Q}^-$  in a bacterial RC or  $\text{P700}^+\text{A}_1^-$  in PS I [30]. Dashed curve in Fig. 1 shows the spin-polarized spectrum of the Zn-substituted bacterial RC depicted from Fuchsle et al. [30]. The E/A/E peak separations of  $\text{CN}^-$ -treated core complex are remarkably larger than those of bacterial RC, and the peak width of each of the E/A/E peaks is also broader than those observed in PS I and the bacterial RC [18]. In the high magnetic field side, an additional absorption spectrum was observed, which was detected neither in the bacterial RC nor in PS I. The spin-polarized spectrum acquired at  $45 \mu\text{s}$  after the laser flash shows that this high field absorption peak become smaller

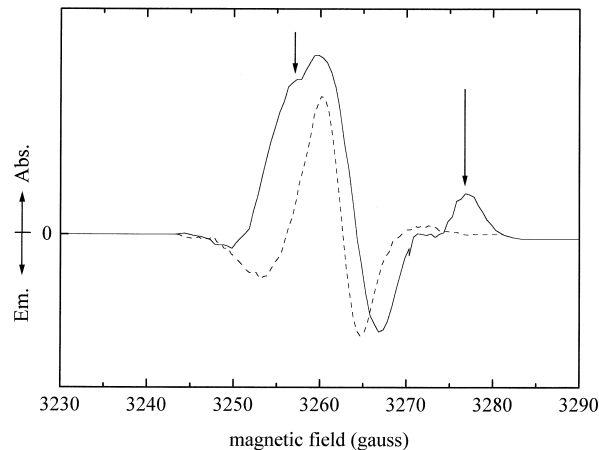


Fig. 1. Spin-polarized transient EPR signal with non-Boltzmann distribution for  $\text{CN}^-$ -treated PS II core complexes. The solid curve shows a smoothed experimental values of the 500 accumulated peak intensities recorded at  $25 \mu\text{s}$  after laser flashes at the varying fixed magnetic field. The spectrum was integrated and the positive intensity shows an absorption signal (A) and the negative one show emission signals (E). The dashed curve shows the spin-polarized spectrum of the Zn-substituted bacterial RC observed by Fuchsle et al. (see Fig. 2 in ref. [30]). The arrow show the  $(\text{P680}^+\text{Phe}^-)^{\text{T}}$  triplet peaks. EPR conditions: Microwave frequency, 9.14 GHz; modulation frequency, 100 kHz; modulation width, 3 G; microwave power 0.2 mW; time constant  $10 \mu\text{s}$ . The start time for data acquisition was approximately  $25 \mu\text{s}$  after the laser flash. Measurement temperature is 80 K.

(data not shown). Another absorption peak at 3257 G seems to overlap on the A peak due to the  $\text{P680}^+\text{Q}_\text{A}^-$  radical pair spectrum of  $g = 2.001$   $\Delta H = 10$  G.

For  $\text{CN}^-$ -treated core complex, with increasing laser flashes, a stable  $\text{Q}_\text{A}^-$  signal intensity gradually increased concomitant with decrease in peak intensity of the transient  $\text{P680}^+$  observed at  $100 \mu\text{s}$  after the laser flash. The similar decrease of  $\text{P680}^+$  signal intensity has been also observed in untreated PS II membranes [8]. In some center with  $\text{Q}_\text{A}^-$  reduced, there may be considered to be three possible origins for the additional absorption peaks;  $\text{P680}^{\text{T}}$ ,  $(\text{P680}^+\text{Phe}^-)^{\text{T}}$ , and  $\text{Phe}^-\text{Q}_\text{A}^-$  radical pair [31]. For PS II membranes with  $\text{Q}_\text{A}^-$  doubly reduced, the  $\text{P680}^{\text{T}}$  triplet signal was reported during illumination at low temperature and the absorption Y triplet peaks were observed near  $g \approx 2$  which has a separation of 120 G much larger than that observed here [31]. On the other hand, the possibility of the radical pair of  $\text{Phe}^-\text{Q}_\text{A}^-$  can be neglected because the radical pair

will give a doublet signal with much less intensity due to non-spin polarization [31]. Therefore, the most probable candidate for the additional doublet peaks may be A/A peaks of  $(P680^+Phe^-)^T$  as observed in the PS II [32]. These signal peaks will not interfere with the ESEEM of the spin polarized radical pair of  $P680^+Q_A^-$  because of their different resonant conditions. After the high yield spin polarized signal decayed with the time constant of  $30 \mu\text{s}$ , we could observe the low yield signal derived from Boltzmann distribution as shown in Fig. 2. The signal intensity of the spin-polarized signal was about 20 times larger than that of the signal with Boltzmann distribution.

Fig. 2 shows a derivative line shape of the light-induced transient EPR signal peak recorded with a time

constant  $100 \mu\text{s}$ , after Boltzmann distribution had been attained. The inset shows the time variation of the signal accumulated at  $100 \mu\text{s}$  after the laser flash at the field position shown by the arrow in the derivative curve and its decay time constant  $t_{1/e}$  was about 3 ms. Each point of the derivative curve indicates the average value of peak intensities of the transient signal induced by laser flashes at varying magnetic field by a step of 0.5 G. The signal plotted versus magnetic field strength has a peak to peak width of about 10 G around  $g = 2.0035$ .

These experiments shows that the spin-polarized radical pair signal was generated immediately after the laser flash with non-Boltzmann distribution, and decays with a time constant of about  $30 \mu\text{s}$ . Then

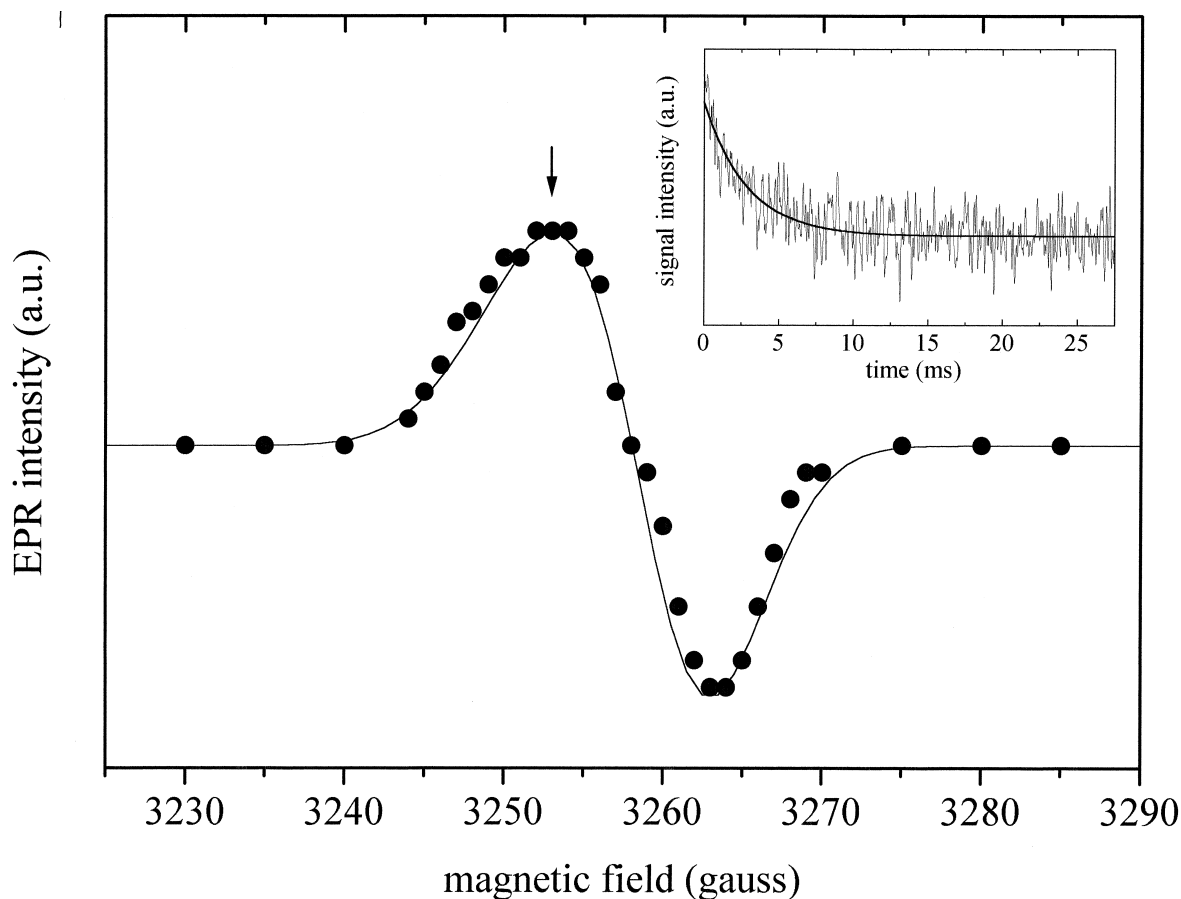


Fig. 2. Transient EPR signal centered at  $g = 2.0035$ , with its width about 10 G. Each point shows the averaged value over 100 accumulated peak intensities at the varying fixed magnetic field recorded at  $100 \mu\text{s}$  after the laser flash in the  $\text{CN}^-$ -treated PS II core complexes. Solid curve shows the calculated values using the parameters  $g = 2.0025$ ,  $\Delta H = 8.5 \text{ G}$  for  $P680^+$  and  $g = 2.0045$ ,  $\Delta H = 10 \text{ G}$  for  $Q_A^-$  with Gaussian line shapes, respectively. Inset: A transient EPR signal observed at the magnetic field indicated by the arrow. Solid curve shows the decay curve fitted with  $t_{1/e} = 3 \text{ ms}$ . EPR conditions: The same as in Fig. 1 except for the time constant  $100 \mu\text{s}$ .

Boltzmann distribution over the spin states was attained, and a rather stable signal with the decay constant about 3 ms was induced. The  $g$ -value and line width  $\Delta H$  for  $P680^+$  and  $Q_A^-$  radical were reported; 2.0025 and  $8.5 \pm 1.0$  G [33], and 2.0045,  $9.5 \pm 0.5$  G [16], respectively. The solid curve in Fig. 2 shows the simulated curve using the parameters  $g = 2.0025$ ,  $\Delta H = 8.5$  G for  $P680^+$  and  $g = 2.0045$ ,  $\Delta H = 10$  G for  $Q_A^-$  with Gaussian line shapes, respectively, fits well with the experimental line shape. Therefore, both of the obtained transient spectra can be ascribed to the  $P680^+Q_A^-$  radical pair, the one to a spin-polarized signal at an earlier time and the other to that with Boltzmann distribution at a later time.

The echo signals measured as a function of time  $\tau$  between two microwave pulses for the  $CN^-$ -treated and Zn-substituted core complexes and the DBMIB-reconstituted PS II RC complex at 80 K were shown in Fig. 3. These spectra were observed at 3440 G ( $g \cong 2.0040$ ), where the yield of the out-of phase signal was maximum. With increasing laser flashes, the echo signals decreased due to electron donation to  $P680^+$  by cyt b559 or Chl. After about 500 laser flashes were given to the sample (the steady state  $Q_A^-$  signal intensity increased), the sample tube was removed from the cavity resonator and then equilibrated at 273 K in the dark for 30 min. These processes were repeated several times during experiments.

For the analysis of ESEEM spectrum, the echo amplitude during the dead time was restored using a parabola interpolation because the initial echo amplitude should be zero according to Eq. (4) based on the theory [22]. A linear interpolation gives almost the same results [19]. In all the three samples, no changes in echo modulation frequency were observed between 80 K and 200 K (data not shown). The results indicate that there are almost no change in the distance between  $P680^+$  and  $Q_A^-$  in this temperature range. The relaxation time  $T_2$  was evaluated to be  $500 \pm 10$  ns for  $CN^-$ -treated core complex,  $400 \pm 10$  ns for Zn-substituted core complex and  $300 \pm 10$  ns for DBMIB-reconstituted PS II RC complex, respectively, by the analysis based on Eq. (4). The small values of  $T_2$  have made the detection of  $P680^+$  signal by pulsed EPR difficult compared to  $P700^+$  in PS I RC ( $T_2 = 1000 \pm 10$  ns [19]) or to  $P860^+$  in bacterial RC ( $T_2 \approx 1000$  ns [18]).

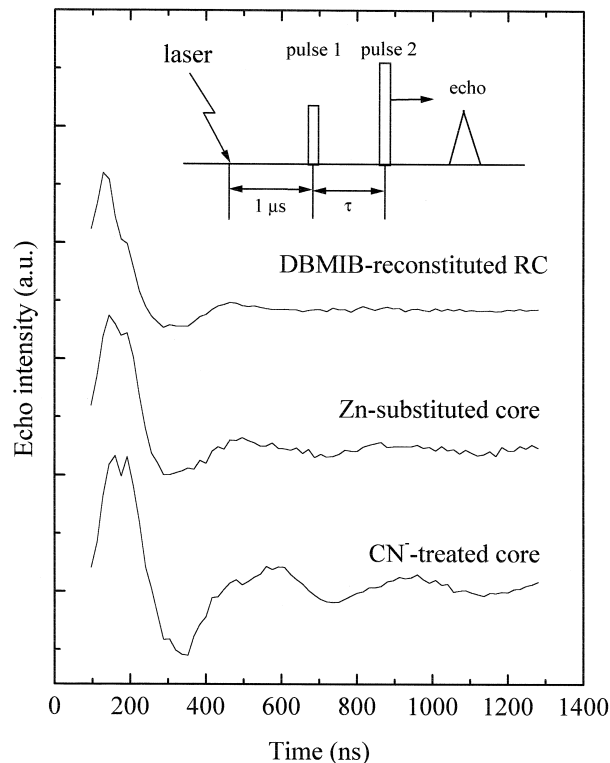


Fig. 3. Primary echo signal of  $P680^+Q_A^-$  as a function of time  $\tau$  between two microwave pulses in DBMIB-reconstituted PS II RC complex, Zn-substituted and  $CN^-$ -treated PS II core complexes observed at 80 K. The vertical positions of curves are arbitrarily shifted. The pulse sequence used in this measurement is shown in the above. The magnetic field was fixed at 3440 G and microwave frequency was 9.66 GHz. See text for details.

A sine Fourier transformation of the traces in Fig. 3 is shown in Fig. 4. The dipolar and exchange interactions influence the position of the two pronounced peaks and the total spectral width. The peaks are assigned to perpendicular orientation of the radius vector connecting the radical species,  $\theta = 90^\circ$ , with respect to the magnetic field orientation. The spectral edges are assigned to the parallel orientation,  $\theta = 0^\circ$ . The positions in frequency corresponding to these perpendicular and parallel orientations are presented by following relations [18] derived from Eq. (4).

$$f_{\perp} = \pm \left( \frac{2D}{3} + 2J \right)$$

$$f_{\parallel} = \pm \left( -\frac{4D}{3} + 2J \right) \quad (5)$$

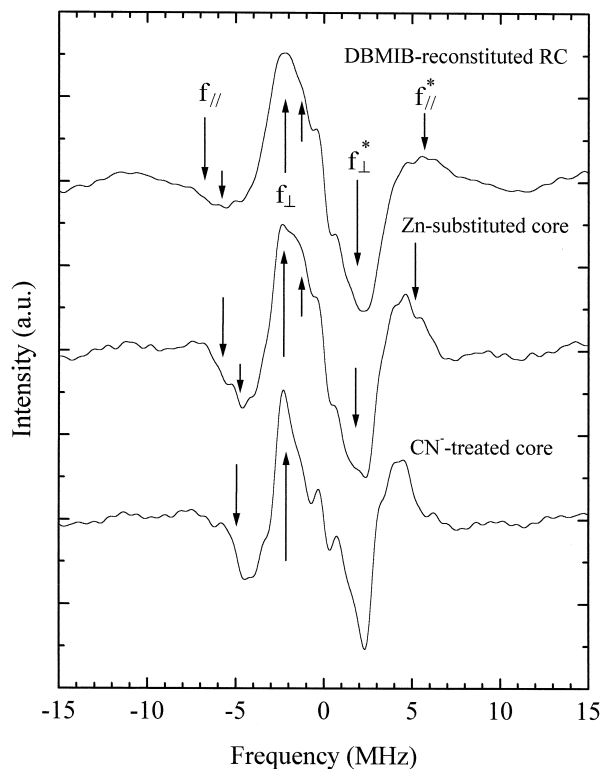


Fig. 4. Results of a sine Fourier transformation of the time domain spectra shown in Fig. 1. The obtained frequency spectra resemble very well the theoretical ones calculated for spin-polarized radical pair coupled by dipolar and exchange interaction (see Fig. 4 in Ref. [18]). The spectral edges correspond to the parallel orientation of the vector connecting the radical pair to the external magnetic field ( $f_{//}$ ), while two peaks reflect singularities appearing for the perpendicular orientation ( $f_{\perp}$ ).

where  $D = 3g\beta/2r^3$  is the dipolar coupling and  $J$  represents the spin exchange coupling constant, respectively.

The obtained lineshape in the frequency domain in the  $\text{CN}^-$ -treated core complex is in a good agreement with the theoretical one (see Fig. 4 in ref. [18]). In the DBMIB-reconstituted RC complex and Zn-substituted core complex, the linewidths were rather broad. The center peaks around  $\pm 0.3$  MHz are artificial Fourier transform peaks due to incomplete background subtraction. Furthermore, the relaxation rate  $1/T_2$  of the  $\text{CN}^-$ -treated core complex was slower than those of the Zn-substituted core and DBMIB-reconstituted RC complexes. These results suggest that the quinones in the Zn-substituted core complex and DBMIB-reconstituted RC complex are in less rigid

structural environment of the quinone binding site than in that in the  $\text{CN}^-$ -treated core complex. The differences may be attributed to the inhomogeneous structural environments caused by the rigorous treatments or to the partial displacement of quinone site from the original  $\text{Q}_A$ -binding locus in the RC complexes. Some quinones may bind to different but still active sites for radical pair formation in the DBMIB-reconstituted RC complex [26]. In the Zn-substituted core complex, about 80% of  $\text{Fe}^{2+}$  were estimated to be substituted by  $\text{Zn}^{2+}$ . Some sites remained just iron depleted that also contributed to the ESEEM. In the  $\text{CN}^-$ -treated core complex, the cyanide binds to  $\text{Fe}^{2+}$  by more than 80% [16], on which sites only we could observe the radical pair signal.

In the Zn-substituted and DBMIB-reconstituted PS II samples, two different sites for quinone binding seems to be suggested from the ESEEM spectra. On the other hand, in the  $\text{CN}^-$ -treated sample, we have observed only one quinone site. This result indicates that the  $\text{CN}^-$ -treated core complex has more rigid and less modified structure of the quinone binding site compared to that for the other preparations. In the Zn-substituted and DBMIB-reconstituted samples, we can assign the outer peaks and the outer spectral edges to one pair and the inner peaks and edges to the other. Thus we have derived two sets of spin–spin coupling parameters.

Table 1. shows the values of frequencies obtained from Eq. (5) using Fig. 4. Two sets of parameters were derived for  $\text{P680}^+\text{Q}_A^-$  radical pair signals in the Zn-substituted and DBMIB-reconstituted samples; (1.42, 1.55) G and (1.14, 1.21) G for  $D$  values and  $-(0.07, 0.13)$  G and  $-(0.11, 0.17)$  G for  $J$  values, respectively. The corresponding distances between

Table 1

Results of frequencies of parallel and perpendicular peaks from Fig. 2 and obtained interaction parameters by Eq. (5). The distances were derived by dipolar interaction parameter for  $\text{P680}^+\text{Q}_A^-$

	$\text{CN}^-$ -treat.	Zn-sub.	RC + DBMIB		
$f_{//}$ (MHz)	5.4	5.7	4.9	6.5	5.5
$f_{\perp}$ (MHz)	2.3	2.3	1.5	2.2	1.3
$D$ (Gauss)	1.38	1.42	1.14	1.55	1.21
$J$ (Gauss)	-0.05	-0.07	-0.11	-0.13	-0.17
$R$ (Å)	27.2	26.9	28.9	26.2	28.4

(error: about 3%).

$P680^+$  and  $Q_A^-$  are derived to be  $27 \text{ \AA}$  and  $29 \text{ \AA}$ , respectively. The spectra of outer set of frequencies have higher yields than those of the inner set. Therefore, the plastoquinone  $Q_A$  in the original position is considered to be responsible for the outer set. The larger distances of  $28.4$  and  $28.9 \text{ \AA}$  for the inner sets may be attributable to the inhomogeneity of the  $Q_A$  positions in the Zn-substituted core complex and the DBMIB-reconstituted PS II RC complexes [2] caused by the rigorous treatment. However, the major components in these three samples gave almost similar distance of  $26.2$ – $27.2 \text{ \AA}$ . In the DBMIB-reconstituted RC and Zn-substituted core complexes, some structural changes might have occurred around the  $Fe^{2+}$  ion and/or quinone binding sites might have been modified in some reaction centers.

The obtained values are close to the distance between  $P860$  and  $Q_A$  ( $\sim 26 \text{ \AA}$ ) in the bacterial RCs [18] and to that estimated in the model calculation of PS II presented by Svensson et al. [34]. The approximate value of  $23$ – $27 \text{ \AA}$  for  $P680$  and  $Fe$  separation was derived from the analyses of a microwave power saturation of  $P680^+$  transient signal in a previous work [8], which was also consistent with the value determined in this experiment. For a recent ESEEM study of PS I, we determined the dipolar and exchange interaction to be  $D = 1.71 \text{ G}$  and  $J = -0.01 \text{ G}$ , respectively [19]. This  $D$  value is larger than that in PS II and gives a little shorter distance of  $25 \text{ \AA}$  between  $P700^+$  and  $A_1^-$  (phyloquinone) [19]. The larger distance in PS II may be a cause of the slower recombination rate between  $P680^+$  and  $Q_A^-$  ( $t_{1/2} = 3 \text{ ms}$  [6]) which is ten-times of that between  $P700^+$  and  $A_1^-$  (phyloquinone) in PS I ( $t_{1/2} = 0.2 \text{ ms}$  [35]). On the other hand, the results in the present study indicate that the radical pair distances in PS II and a purple bacterial RC are similar [18], though the recombination rate is faster in PS II than that in the purple bacterial RC by ten times. This difference may be attributable to a difference between their local structure such as spin density distribution over the dimer chlorophyll's [36,37].

Fig. 5 shows the decay kinetics of ESE signal for the radical pairs in the three PS II preparations. The decay rates were  $35.8 \mu\text{s}$  ( $CN^-$ -treated core complex),  $44.3 \mu\text{s}$  (Zn-substituted core complex) and  $32.5 \mu\text{s}$  (DBMIB-reconstituted PS II RC), respectively. The value of about  $35 \mu\text{s}$  is significantly shorter than that

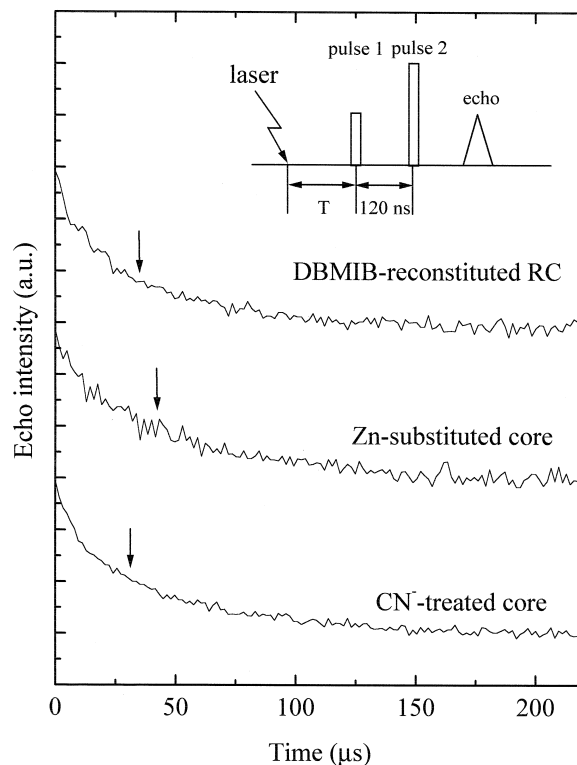


Fig. 5. ESE signal with varying delay time  $T$  after the laser flash, for a 2-pulse echo sequence. DBMIB-reconstituted RC complex (top), Zn-substituted (middle) and  $CN^-$ -treated (bottom) PS II core complexes. The vertical positions of curves are arbitrarily shifted. The arrows indicate the  $t_{1/e}$  of decay. The pulse sequence used in this measurement is also shown. The measurement temperature is  $80 \text{ K}$ . The magnetic field was fixed at  $3440 \text{ G}$  and microwave frequency was  $9.66 \text{ GHz}$ .

obtained in the actual  $P680^+Q_A^-$  recombination time observed by the transient CW EPR method in this work, by a fluorescence measurement in the untreated PS II ( $3$ – $5 \text{ ms}$  [4]) and by an absorption change of  $P680$  in the DBMIB-reconstituted RC complex ( $11 \text{ ms}$  [17]). The cause of the discrepancies is not clear but may be partially due to a fast spin relaxation specific for the spin polarized ESE signal, such as a cross relaxation between  $|T_0\rangle$  and  $|S\rangle$  levels. Similar shortening of the decay rates was also found in PS I RC [19].

In conclusion, the distance between  $P680$  and the acceptor  $Q_A$  in PS II RC has been determined for the first time by analysis of ESEEM spectra of the spin-polarized radical pairs to be  $27.2 \pm 1.0 \text{ \AA}$ .

This work was supported by Grant-in Aid on



General Research (06452073) to A. K., on Priority-Area-Research to S.I.: “Photoreaction Dynamics” (08218261), “Decoding Earth Evolution Program” (08228225), “Biometalics” (08249244), and “Single Electron Devices” (08247216) from the Ministry of Education, Science, Sports and Culture Japan. H. H acknowledges a support by the Sasakawa Scientific Research Grant from the Japan Science Society. S.A.D. acknowledges a fellowship for Priority-Area Research from Japan Society for Promotion of Science (JSPS).

## References

- [1] M.R. Wasierewski, D.G. Johnson, M. Seibert, Govindjee, *Proc. Natl. Acad. Sci. U.S.A.* 86 (1989) 524–528.
- [2] P. Mathis, A.W. Rutherford, in: J. Ames (Ed.), *Photosynthesis*, Elsevier, Amsterdam, 1987, 63–96.
- [3] A. Joliot, *Biochim. Biophys. Acta* 357 (1974) 439.
- [4] S. Reinman, P. Mathis, *Biochim. Biophys. Acta* 635 (1981) 249–258.
- [5] P. Mathis, A. Vermeglio, *Biochim. Biophys. Acta* 368 (1974) 130–134.
- [6] P. Mathis, A. Vermeglio, J. Haveman, *Lasers in Physical Chemistry and Biophysics*, Elsevier, Amsterdam, 1976, pp. 465–474.
- [7] C.A. Buser, L.K. Thompson, B.A. Diner, G.W. Brudvig, *Biochemistry* 26 (1990) 8977–8985.
- [8] Y. Kodera, K. Takura, A. Kawamori, *Biochim. Biophys. Acta* 1101 (1992) 23–32.
- [9] J.H.A. Nugent, B.A. Diner, M.C.W. Evans, *FEBS Lett.* 124 (1981) 241–244.
- [10] H. Michel, O. Epp, J. Deisenhofer, *EMBO J.* 5 (1986) 2445–2451.
- [11] P.J. Hore, D.A. Hunter, C.D. McKie, A.J. Hoff, *Chem. Phys. Lett.* 137 (1987) 495–500.
- [12] D. Stehlik, C.H. Bock, J. Peterson, *J. Phys. Chem.* 93 (1989) 1612–1619.
- [13] A.J. Hoff, P. Gast, J.C. Romijn, *FEBS Lett.* 73 (1977) 185–196.
- [14] T. Nagatsuka, S. Fukuhara, K. Akabori, Y. Toyoshima, *Biochim. Biophys. Acta* 1057 (1991) 223–231.
- [15] S. Kuroiwa, PhD thesis, Hiroshima University, 1996.
- [16] Y. Sanakis, V. Petrouleas, B.A. Diner, *Biochemistry* 33 (1994) 9922–9928.
- [17] S. Itoh, M. Iwaki, T. Tomo, K. Satoh, *Plant Cell Physiol.* 37 (1996) 833–839.
- [18] S.A. Dzuba, P. Gast, A.J. Hoff, *Chem. Phys. Lett.* 236 (1995) 595–602.
- [19] S.A. Dzuba, H. Hara, A. Kawamori, M. Iwaki, S. Itoh, Yu.D. Tsvetkov, *Chem. Phys. Lett.* 264 (1997) 238–244.
- [20] T.O. Yeates, H. Komiya, D.C. Rees, J.P. Allen, G. Feher, *Proc. Natl. Acad. Sci. U.S.A.* 84 (1987) 6438–6442.
- [21] P. Fromme, H.T. Witt, W.D. Schubert, O. Klukas, W. Saenger, B. Krauß, *Biochim. Biophys. Acta* 1275 (1996) 76–83.
- [22] J. Tang, M.C. Thurnau, J.R. Norris, *Chem. Phys. Lett.* 219 (1994) 283–290.
- [23] J. Tang, M.C. Thurnau, A. Kubo, H. Hara, A. Kawamori, *J. Chem. Phys.* 160 (1997) 7471–7478.
- [24] O. Nanba, K. Satoh, *Proc. Natl. Acad. Sci. U.S.A.* 84 (1987) 109–112.
- [25] K. Satoh, H. Nakane, Refined purification and characterization of the D1-D2 reaction center of Photosystem II, in: M. Baltscheffsky (Ed.), *Current Research in Photosynthesis*, vol. I, Kluwer Academic Publishers, Dordrecht, pp. 271–274.
- [26] H. Nakane, M. Iwaki, K. Satoh, S. Itoh, *Plant Cell Physiol.* 32 (1991) 1165–1171.
- [27] T. Kuwabara, N. Murata, *Plant Cell Physiol.* 23 (1982) 533–539.
- [28] D.F. Ghanotakis, D.M. Demetriou, C.F. Yocum, *Biochim. Biophys. Acta* 891 (1987) 15–21.
- [29] V.V. Klimov, E. Dolan, E.R. Shaw, B. Ke, *Proc. Natl. Acad. Sci. U.S.A.* 77 (1980) 7227–7231.
- [30] G. Fuchsle, R. Bittl, A. van der Est, W. Lubitz, D. Stehlik, *Biochim. Biophys. Acta* 1142 (1993) 23–35.
- [31] F.J.E. van Mieghem, W. Nitschke, P. Mathis, A.W. Rutherford, *Biochim. Biophys. Acta* 977 (1989) 207–214.
- [32] M.C.W. Evans, Y.E. Atkinson, R.C. Ford, *Biochim. Biophys. Acta* 806 (1985) 247–254.
- [33] C.W. Hoganson, G.T. Babcock, *Biochemistry* 28 (1989) 1448–1454.
- [34] B. Svensson, C. Etchebest, P. Tuffery, P. van Kan, J. Smith, S. Styring, *Biochemistry* 35 (1996) 14486–14502.
- [35] S. Itoh, M. Iwaki, in: N. Mataga, T. Okada, H. Masuhara (Eds.), *Dynamics and Mechanisms of Photoinduced Electron Transfer and Related Phenomena*, Elsevier, Amsterdam, 1992, pp. 527–540.
- [36] S.E.J. Rigby, J.H.A. Nugent, P.J. O’Malley, *Biochemistry* 33 (1994) 10043–10050.
- [37] M. Huber, R.A. Isaacson, E.C. Abresch, D. Gaul, C.C. Schenck, G. Feher, *Biochim. Biophys. Acta* 1273 (1996) 108–128.